

## Optical Dielectric Strength of Alkali-Halide Crystals Obtained by Laser-Induced Breakdown\*

Eli Yablonovitch<sup>†</sup>

*Gordon McKay Laboratory, Harvard University, Cambridge, Massachusetts 02138*

(Received 16 August 1971)

CO<sub>2</sub> laser-induced breakdown was studied in ten of the alkali halides. The bulk intrinsic breakdown thresholds are intimately related to the corresponding dc dielectric strengths. It is therefore concluded that the same mechanism is operative in both types of experiment. A method is proposed for designing more damage-resistant materials. In addition, the question of inclusions is dealt with.

Laser-induced breakdown<sup>1</sup> in transparent dielectrics has been studied since high-intensity optical fields have become available. Nevertheless, it has not been possible to ascertain the intrinsic bulk damage mechanism of the optical crystals. Complications from self-focusing,<sup>2</sup> and multiphoton and cascade ionization of impurities<sup>3</sup> are responsible for this.

The much longer wavelength of the CO<sub>2</sub> laser compared to visible and near ir lasers offers certain advantages. Since the critical power for self-focusing varies as wavelength squared, this effect will be absent at the power levels considered here. Moreover, multiphoton ionization of impurities or its low-frequency limit,<sup>4</sup> tunnel ionization, is also absent.

Ten members of the alkali-halide family were studied. Over the years, considerable work has been done on the dc dielectric strength<sup>5</sup> of these crystals as prototype insulators. Their threshold for laser-induced breakdown is of practical importance for their application as optical materials in the new ultrahigh peak-power CO<sub>2</sub> lasers.<sup>6</sup>

The source of radiation was a CO<sub>2</sub> laser of the TEA type<sup>7</sup> with a helical electrode structure, emitting pulses at the 10.6- $\mu$ m wavelength. The laser was known to be operating in the lowest-order transverse Gaussian mode. There were several longitudinal modes, however, which contributed a time structure to the pulse, periodic at the cavity round-trip time. A typical laser pulse is shown in Fig. 1(a). The output of a fast ir detector is displayed, the time structure being fully resolved. The phase relationships between the longitudinal modes varied from shot to shot, changing the details of the time structure and causing the peak of the envelope to fluctuate by  $\pm 15\%$ .

Successive laser shots (1/sec) were focused into bulk single crystals using a 1-in. focal length "Irtan 2" lens. The breakdown was monitored by observing the visible light from the focal region and by examining the damaged region under the microscope. It was found that most of the crystals suffered some damage even at relatively low power levels. The threshold for this type of damage varied by an order of magnitude from one position in the crystal to another. At any particular energy level, damage would occur on the first laser shot or not at all. Spatial inhomogeneities rather than statistical

fluctuations are therefore responsible.<sup>8</sup> Figure 2(a) shows that these spatial inhomogeneities are in fact inclusions. The damage bubbles occur randomly near, not necessarily in, the tiny focal volume. At a well-defined power threshold, an elongated pointed bubble forms, its vertex falling at the focus [Fig. 2(b)]. This power level is regarded as the bulk intrinsic breakdown threshold. Its value is reproducible in crystals from different manufacturers, with inclusions or without. When no inclusion-free samples of a compound were available, the considerations mentioned above were used to determine the dielectric strength.

Figures 1(b) and 1(c) show the transmission of laser radiation through the focus at two different points in an inclusion-free sample of KCl. The incident intensity was near threshold and, at one position, breakdown took place on the first laser shot [Fig. 1(b)]. At the other position, three shots were required [Fig. 1(c)]. The third trace was drawn heavier for emphasis. As can be seen, the peak of the pulse envelope was higher on the third shot than on the first two. Since this behavior is typical, it implies that the threshold power level occurs at the peak of the pulse envelope. The arrow in Fig. 1(c) indicates the position in the third pulse train where the breakdown is thought to have occurred. From the width of that peak, we may conclude that the breakdown develops in a time shorter than a few nanoseconds.

The  $1/e^2$  diameter<sup>9</sup> of the focal spot was  $2\omega_0 = 50 \mu\text{m}$ . The length<sup>9</sup> of the focal region was  $n \times 2z_0$ , or about 600  $\mu\text{m}$  for an index of refraction  $n = 1.5$ . Spherical aberration from the lens was negligible in this geometry.

TABLE I. The dielectric strength of the alkali halides at the CO<sub>2</sub> laser frequency and at dc (in units of  $10^6$  V/cm). The accuracy is  $\pm 10\%$ .

		F	Cl	Br	I
CO <sub>2</sub> laser	Na	...	1.95	0.91	0.79
	dc <sup>a</sup>	2.40	1.50	0.83	0.69
CO <sub>2</sub> laser	K	2.40	1.39	0.94	0.72
	dc <sup>a</sup>	1.80	1.00	0.69	0.57
CO <sub>2</sub> laser	Rb	...	0.93	0.78	0.63
	dc <sup>a</sup>	...	0.83	0.58	0.49

<sup>a</sup>The dc dielectric strength is taken from A. von Hippel [J. Appl. Phys. 8, 815 (1937)].

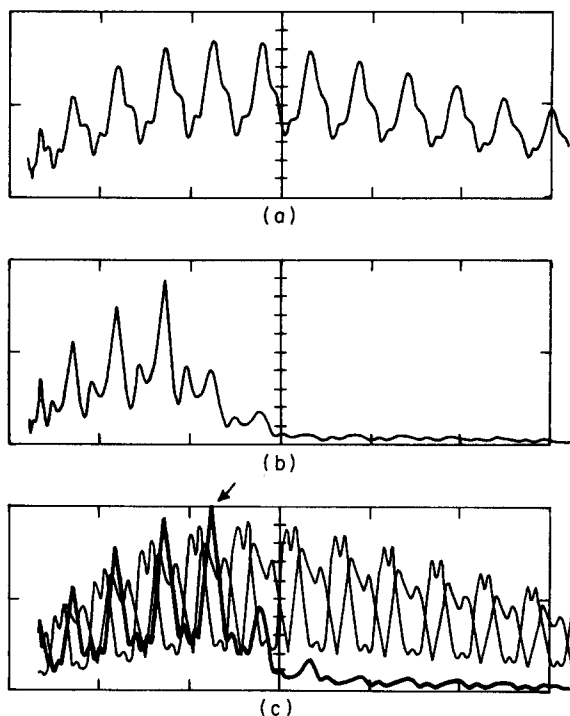


FIG. 1. The time scale is 20 nsec/div. (a) Typical laser pulse. (b) The transmission of radiation through the focus. Breakdown on the first shot. (c) Breakdown after three shots. The third trace is drawn heavier. The arrow indicates where the breakdown occurred.

Table I shows the experimental results. The threshold is given in terms of the rms electric field at the most intense point in the focus. Its level is defined as the electric field at which the probability of breakdown is 50%. In the best crystal studied, the breakdown field was spatially homogeneous within  $\pm 5\%$ .

The comparison in Table I between the dc and CO<sub>2</sub> laser breakdown fields is striking.<sup>10</sup> The variations throughout the Periodic Table are the same in both cases, with the absolute value of the laser data being roughly 25% higher. Unfortunately, it is incorrect to make a direct comparison of the *absolute* values of these two sets of results. The dc dielectric strength is known to depend very weakly on both sample thickness<sup>11</sup> and the rise time<sup>12</sup> of electric field. Correspondingly, the laser-induced breakdown probably has a weak dependence on focal volume due to electron diffusion. Impact ionization theories,<sup>1,5</sup> which ignore these effects, predict that  $E_{\text{rms}}(\omega) = (1 + \omega^2\tau^2)^{1/2}E_{\text{dc}}$ , where  $\omega$  is the laser frequency and  $\tau$  is an electron-optical-phonon collision time. For these materials  $\omega\tau \approx 1$ .

The fields in Table I were measured at room temperature. Raising the temperature of a KCl crystal to 200 °C resulted in a 10% increase in breakdown field. This is consistent with pulsed dc results.<sup>12</sup> There was no measurable anisotropy of the breakdown field.

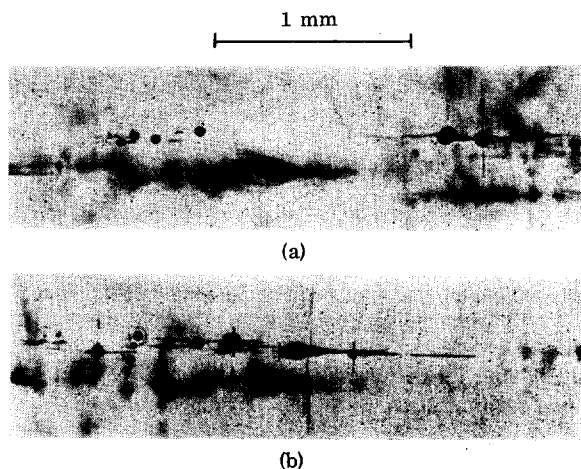


FIG. 2. Two damaged regions in a crystal with a moderately high density of inclusions. The round black objects are bubbles. The radiation, incident from left to right, was just at the intrinsic breakdown threshold. In one case (a) there was damage only at the inclusions. In (b), intrinsic breakdown occurred as evidenced by the pointed bubble. The straight lines represent cleavage.

If, as these experiments indicate, the dc and CO<sub>2</sub> laser breakdown are similar, then it should be possible to design more damage-resistant optical materials. The dc dielectric strength is known to increase when lattice disorder is introduced, as in ternary mixed crystals.<sup>13</sup> A factor of 3 in electric field or about 10 in intensity should be possible. This applies, of course, to bulk rather than surface damage.

In view of the fact that electric breakdown represents a fundamental instability of the system of electrons and background lattice, further theoretical work on this subject is warranted.

The author would like to thank Professor N. Bloembergen for his guidance and encouragement in this work.

\*Supported under Army Research Projects Agency Contract No. DAHC-15-67-C-0219.

<sup>†</sup>Predoctoral Fellow of the National Research Council of Canada.

<sup>1</sup>G. M. Zverev, T. N. Mikhailova, V. A. Pashkov, and N. M. Solov'na, Zh. Eksperim. i Teor. Fiz. 53, 1849 (1967) [Sov. Phys. JETP 26, 1053 (1968)].

<sup>2</sup>S. A. Akhmanov, A. P. Sukhorukov, and R. V. Khokhlov, Usp. Fiz. Nauk 93, 19 (1967) [Sov. Phys. Usp. 10, 609 (1968)].

<sup>3</sup>R. W. Hellwarth, in *Damage in Laser Materials*, edited by A. J. Glass and A. H. Guenther, Natl. Bur. Std. (U.S.). Special Publication No. 341 (U.S. Dept. of Commerce, Washington, D. C., 1970), p. 67.

<sup>4</sup>L. V. Keldysh, Zh. Eksperim. i Teor. Fiz. 47, 1945 (1964). [Sov. Phys. JETP 20, 1307 (1965)].

<sup>5</sup>For a review see J. J. O'Dwyer, *The Theory of the Dielectric Breakdown of Solids* (Oxford U. P., London, 1964).

<sup>6</sup>R. Dumanchin, M. Michon, J. C. Farcy, G. Boudinet, and J. Rocca-Serra, Laser Focus 7, 32 (1971).

<sup>7</sup>A. J. Beaulieu, Appl. Phys. Letters 16, 504 (1970).

<sup>8</sup>M. Bass and H. H. Barrett, in Proceedings of a Symposium on Damage in Laser Materials (to be published).

<sup>9</sup>A. Yariv, *Quantum Electronics* (Wiley, New York, 1967), Chap. 14.

<sup>10</sup>Ruby-laser-induced breakdown in the same materials does not show any systematic behavior, and is not

entirely reproducible [D. Olness, *J. Appl. Phys.* 39, 6 (1968)].

<sup>11</sup>J. J. O'Dwyer, *J. Phys. Chem. Solids* 28, 1137 (1967).

<sup>12</sup>F. W. Kasetta and H. T. Li, *J. Appl. Phys.* 37, 2744 (1966).

<sup>13</sup>A. von Hippel and G. M. Lee, *Phys. Rev.* 59, 820 (1941).

APPLIED PHYSICS LETTERS

VOLUME 19, NUMBER 11

1 DECEMBER 1971

## *pn*-Schottky Hybrid Cold-Cathode Diode

C. A. Stolte and R. J. Archer

*Hewlett-Packard Laboratories, Palo Alto, California 94304*

(Received 19 July 1971)

The device is a forward-biased GaAs<sub>0.6</sub>P<sub>0.4</sub> *pn*-junction diode whose thin *p* layer is coated with a cesiated film of either Ag or Au 100–300 Å thick. In some cases the diodes are heat treated at 250 °C before cesiation. A cathodic emission efficiency of 1.4% is obtained at 10 A cm<sup>-2</sup> for a heat-treated diode with a 100-Å-thick Au film. The emission is uniform over the coated surface and is proportional to exp(*qV*/*kT*). Preliminary data indicate long life for the device when operated in an ambient of Cs vapor.

A cold-cathode diode has been developed which is a hybrid of Schottky barrier<sup>1,2</sup> and *pn*<sup>3,4</sup> cold-cathode diodes. The device is a GaAs<sub>0.6</sub>P<sub>0.4</sub> *pn* junction whose thin *p* layer is coated with a very thin metal film that is covered in turn with a monolayer of Cs. The new structure is compared with the two simpler diodes in Fig. 1. It obviates two problems of the simple diodes, namely, (1) the small magnitudes of practical Schottky-barrier heights, and (2) the processing difficulties associated with obtaining the chemically clean surfaces required for cesiating the *pn* device. The effective Schottky-barrier height for the hybrid device is approximately the energy gap of the degenerately doped *p* layer, about 1.9 eV for the devices described here. The clean metal surface for cesiation is obtained, as in the Schottky diode case, by *in situ* evaporation of the thin metal layer.

The emission efficiency — defined as the ratio of the anode current to the total diode current — is expected to be given by

$$\eta = F_d \gamma [\text{sech}(w/L_n)] F_t F_c,$$

where  $F_d$  is the fraction of the total current that is minority-carrier diffusion current;  $\gamma$  is the fraction of the diffusion current that results from electron injection into the *p* layer;  $\text{sech}(w/L_n)$  is the fraction of the electrons that diffuse across the *p* layer without recombining, where  $w$  is the thickness of the *p* skin and  $L_n$  is the diffusion length of electrons;  $F_t$  is the fraction of the electrons impinging on the space-charge layer which are emitted into vacuum; and  $F_c$  is the fraction of the *p* surface that is not covered by the comb-shaped contact. The following magnitudes are expected:  $F_d \geq 0.5$  for diode current densities above about 10 A cm<sup>-2</sup> as described below;  $\gamma \geq 0.5$  from experience with light-emitting diodes<sup>5</sup>;  $\text{sech}(w/L_n) = 0.65$  for  $w = L_n = 0.5 \mu\text{m}$ ;  $F_t \approx 1.6 \times 10^{-2}$

is an estimate from the theory given in Sec. 2 of Ref. 1 assuming a Ag film 100 Å thick pulse the assumption of a 30% loss by scattering in the space-charge region at the *p*-metal interface; and  $F_c = 0.8$ . On the basis of these values, efficiencies between 0.2 and 0.8% are predicted.

Planar diodes were formed by Zn diffusion into *n*-type substrates with  $n = 10^{17}$  cm<sup>-3</sup> through openings in a SiN<sub>x</sub> layer. The *p* region has a square cross section 0.043 cm on a side and is about 0.5 μm deep. It is contacted by a Au comb-shaped pattern that covers about 20% of the surface. Deposition of the thin metal layer, cesiation, and cathodic emission measurements are carried out as previously described.<sup>1</sup> After cesiation the metal work functions are approximately 1.4 eV. In some cases the diodes were heated to 250 °C for 10 min after the deposition of the metal film and before cesiation.

Diodes made with Au and Ag films, 100 and 300 Å thick, with and without the 250 °C treatment were studied giving eight permutations. The maximum efficiencies measured at total diode currents between 20 and 100 mA are given in Table I. The highest value, 1.4%, is measured at 10 A cm<sup>-2</sup> for the heat-treated diode with a 100-Å Au film. Magnified imaging of the emitted electrons on a fluorescent screen shows that the emission is uniform over the diode surface. In all cases, the emitted current collected by the anode obeys  $I_A \propto \exp(qV/kT)$ , where  $V$  is the bias applied to the diode less any series voltage drop.

TABLE I. Maximum emission efficiencies (%) at 300°K.

	100 Å	100 Å (250 °C)	300 Å	300 Å (250 °C)
Ag	0.22	0.50	0.06	0.14
Au	0.35	1.40	0.08	0.40